nature physics

REVIEW ARTICLE

PUBLISHED ONLINE: 2 JUNE 2015 | DOI: 10.1038/NPHYS3347

Magnon spintronics

A. V. Chumak*, V. I. Vasyuchka, A. A. Serga and B. Hillebrands

Magnon spintronics is the field of spintronics concerned with structures, devices and circuits that use spin currents carried by magnons. Magnons are the quanta of spin waves: the dynamic eigen-excitations of a magnetically ordered body. Analogous to electric currents, magnon-based currents can be used to carry, transport and process information. The use of magnons allows the implementation of novel wave-based computing technologies free from the drawbacks inherent to modern electronics, such as dissipation of energy due to Ohmic losses. Logic circuits based on wave interference and nonlinear wave interaction can be designed with much smaller footprints compared with conventional electron-based logic circuits. In this review, after an introduction into the basic properties of magnons and their handling, we discuss the inter-conversion between magnon currents and electron-carried spin and charge currents; and concepts and experimental studies of magnon-based computing circuits.

A disturbance in local magnetic ordering can propagate in a magnetic material in the form of a wave. Such a wave was first predicted by F. Bloch in 1929 (ref. 1) and was named a spin wave as it is related to the collective excitations of the electron spin system in ferromagnetic metals and insulators[2,3]. The wide variety of linear and nonlinear spin-wave phenomena boosted interest into the fundamental properties[2–4], while spin waves in the GHz frequency range were of great interest for applications in telecommunication systems and radars[5,6]. Nowadays, spin waves are considered as potential data carriers for computing devices, as they have nanometre wavelengths, can be in the low-THz frequency range, provide Joule-heat-free transfer of spin information over macroscopic distances, and access to wave-based computing concepts (see Box 1)[7–44].

The field of science that refers to information transport and processing by spin waves is known as magnonics[22,45,46]. This name relates to the magnon—the spin-wave quantum associated with the flip of a single spin. The usage of magnonic approaches in the field of spintronics, hitherto dealing with electron-carried spin currents, gave birth to the emerging field of magnon spintronics[47]. The scheme of magnon spintronics in Fig. 1 shows that, besides magnon-based elements operating with analogous and digital data, this field comprises also converters between the magnon subsystem and the electron-carried spin and charge currents. These converters interface the magnonic circuitry with spintronic and electronic environments. The main building blocks of magnon spintronics shown in Fig. 1 are discussed here in the light of their advantages, challenges and perspectives.

Spin-wave basics and toolbox

Two general types of interactions couple electron spins and thus define the spin-wave characteristics: strong but short-distance exchange interactions and relatively weak long-range dipole–dipole interactions. The waves with short wavelength λ (roughly, $\lambda < 1\,\mu$m), whose properties are mostly governed by the exchange interaction, are named exchange spin waves. Correspondingly, the long-wavelength waves are named dipolar or magnetostatic waves (MSWs; refs 2,3). Owing to the inherent anisotropy of the dipolar interaction, the MSWs are classified depending on the angle between the spin-wave wavevector $\mathbf{k}$ and the saturation magnetization $\mathbf{M}$. In an in-plane magnetized magnetic film, waves propagating along and transverse to $\mathbf{M}$ are named backward volume magnetostatic waves (BVMSWs) and magnetostatic surface waves (MSSWs, also known as Damon–Eshbach waves), respectively. Dipolar waves in a normally magnetized film are named forward volume magnetostatic waves (FVMSWs). Historically, most of the magnon-based devices for microwave signals processing[5,6] operate with dipolar spin waves, which can be excited and detected rather conveniently by inductive antennas. Nowadays, attention is more focused on the exchange waves that allow usage in nanometre-sized structures and devices. All these types of waves have different dispersion characteristics (dependencies of the spin-wave frequency f on the wavenumber k)[48] and nonlinear properties, and thus offer specific advantages for data processing[22,45,46].

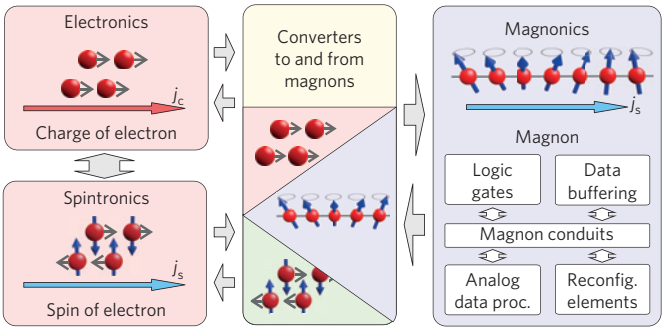

Figure 1 | The concept of magnon spintronics. Information coded into charge or spin currents is converted into magnon currents, processed within the magnonic system and converted back[47].

Spin waves are usually excited in thin films and conduits fabricated in the form of narrow strips of a magnetic material. The most commonly used materials are polycrystalline metallic films of Permalloy (Py, $Ni_{81}Fe_{19}$) (refs 45,46), which combine a relatively low magnetic damping with good suitability for micro-sized patterning; and single-crystal films of yttrium–iron–garnet (YIG, $Y_3Fe_5O_{12}$) (refs 21,22), which possess extremely low damping.

Fachbereich Physik and Landesforschungszentrum OPTIMAS, Technische Universität Kaiserslautern, 67663 Kaiserslautern, Germany.
*e-mail: chumak@physik.uni-kl.de

Box 1 | Data processing benefiting from magnonics.

Wave-based computing. A promising direction for a future beyond-CMOS computing technology (CMOS: complementary metal–oxide–semiconductor) is based on the substitution of electrons by quasi-particles such as magnons or photons[7–9], which allow operations with vector rather than scalar variables. The usage of wave phase provides an additional degree of freedom in data processing[10–13], opens the way to non-Boolean computing algorithms[14,15], and allows a decrease in footprint of the computing elements[16]. A good example is a majority gate produced in the form of a three-input combiner[12,16,17], which substitutes several tens of CMOS transistors. Reversible logic[18,19] and parallel computing, where the same element simultaneously processes data at different frequencies[20], are other advantages.

Insulator-based spintronics. A magnon current has advantages as compared to a conventional spin-polarized electron current. It does not involve the motion of electrons and, thus, it is free of Joule heat dissipation[7]. In low-damping magnetic dielectrics (for example, yttrium-iron-garnet, YIG; ref. 21) magnons can propagate over centimetre distances[22] whereas an electron-carried spin current is limited by the spin diffusing length, which does not exceed one micrometre.

Wide frequency range from GHz to THz. The wave frequency defines the maximum clock rate of a computing device. The magnon spectrum covers the GHz frequency range used nowadays in communication[5,6], and it reaches into the very promising THz range[21,23,24]. For example, the edge of the first magnonic Brillouin zone in YIG lies at about 7 THz (ref. 21).

Nanosized structural elements. The minimal sizes of wave-based computing elements are defined by the wavelength of the used wave. Spin waves are promising because they allow operations with wavelengths below 10 nm (a lower limit is given by the lattice constant of a specific magnetic material[21,23,24]). Moreover, the frequency of exchange magnons increases quadratically with decreasing wavelength, and their group velocity increases linearly in the first one-third of the Brillouin zone. Thus, miniaturization[25,26] of magnon-based devices goes along with an increase in computing speed (see discussions in ref. 7).

Contactless wiring. Wiring, which is required for powering of separate elements, increases the complexity of the architecture and occupies a significant part of the chip area. Feeding of magnonic elements can be realized using an electro-magnetic wave: Au *et al.* proposed placing a magnonic chip in a global microwave field driving a number of separate, local spin-wave transducers[27].

Wide physical toolbox. Magnon properties can be engineered on a broad scale by a choice of the magnetic material, the strength of a magnetic field, the magnetization direction, the geometry of magnetic structures, and so on. In addition, there is a variety of physical effects applicable for the control of spin-wave excitation and propagation. For example, nonreciprocal operations required in communications[28] and logic devices[29] can be realized by the use of the magnetostatic surface waves (MSSWs; refs 2,3): an antenna excites a MSSW packet in one propagation direction only[29–31]. Another example is a spin-wave wavelength converter[32], which uses the change in the geometry of a spin-wave conduit to reduce the magnon wavelength. Spatial addressing of magnon currents is possible even in a plane film: spin-wave caustics[33,34] can be used for the formation of non-diffractive wave beams. The direction of these beams is controlled by the magnetic field.

Nonlinear data processing. A wide variety of pronounced nonlinear spin-wave effects[2–4,22], opens additional opportunities for data processing. For example, data can be transferred over large distances without distortion in the form of spin-wave solitons[35] and bullets[36], or they can be buffered in non-propagating modes and restored afterwards[37]. Effects such as wavefront reversal[36,38] and power limiting[39] have been demonstrated. Finally, the nonlinearity of magnons allows the control of one magnon current by another and, thus, the realization of magnon transistors[7].

Macroscopic quantum phenomena. Magnons are bosons and can form a Bose–Einstein condensate—a spontaneous coherent ground state—established independently of the magnon excitation mechanism even at room temperature[40,41]. A magnon supercurrent, a collective motion of condensed magnons driven by a phase gradient of a condensate wavefunction[42], can be used for low-loss information transfer. Recent theoretical predictions address the magnonic Josephson effect[43] and the magnon Aharonov–Casher effect, where the supercurrent is controlled by an electric field[44].

At the same time, intensive theoretical and experimental research efforts are devoted to the development of novel materials. An example is the class of ferromagnetic Heusler compounds, which combine high spin polarization, high saturation magnetization, and a high Curie temperature with a low magnetic Gilbert damping[49,50]. It has also been shown that CoFeB composites are a good choice for magnonics[51,52]. Finally, recently developed YIG films of nanometre thicknesses[25,53–55] have great potential for application in a nanosized insulator-based magnon spintronics[25,26].

The classical approach for magnon excitation is the inductive microwave technique, where an electromagnetic signal applied to a microwave antenna excites magnetization precession in the magnetic material via an alternating Oersted field induced around the antenna[29–31,56]. Up to now, this technique has retained its importance for application as it allows control of the frequency, wavelength and phase of the injected magnons. Among other methods of magnon excitation we would like to mention optical means, where an ultra-short laser pulse pushes the magnetic system out of equilibrium[46]; parametric amplification of spin waves from thermal fluctuations[22,57]; magneto-electric cells in which an electric field controls an exchange bias field or an anisotropy field in a ferromagnet/multiferroic heterostructure[16,58]; and spin-transfer-torque (STT)-based magnon injection[59–62]. Generally, conversion efficiencies are at present still rather low, but further progress is expected. STT-based magnon injection will be discussed later in more detail as it enables the direct coupling of spin waves with a spin-polarized d.c. electric current and, thus, bridges magnonics with electron-based spintronics and electronics.

Among the most common means to detect magnons, we list the already mentioned antenna-based inductive techniques; optical techniques including time-resolved Faraday and Kerr effects[27,63] and Brillouin light scattering (BLS) spectroscopy[22,64]; caloritronic means, where magnons are measured by their thermal footprint[65,66]; and magnon detection via the spin-pumping effect[53,67–70]. However, probably the most powerful tool for fundamental studies is BLS spectroscopy, as it delivers spatial,

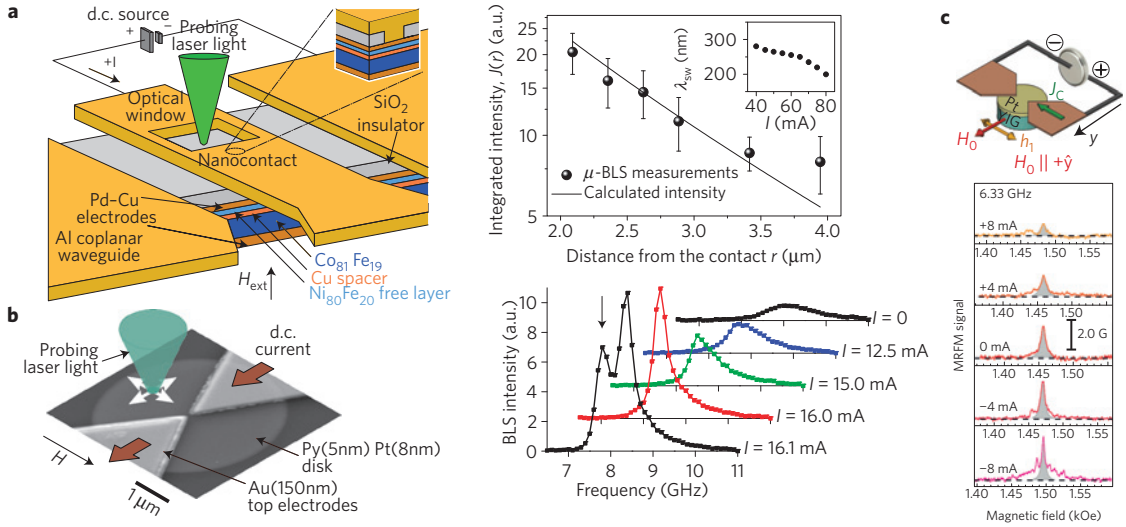

Figure 2 | Magnon excitation by spin-transfer torque. a, Sample layout for studies of propagating spin waves induced by the spin-transfer torque (STT; ref. 60). Right panel: Spin-wave intensity as a function of the distance from the centre of the point contact. The inset shows the dependence of the spin-wave wavelength on the applied d.c. current. **b**, Experimental layout of a magnetic nano-oscillator driven by a spin current generated by the spin Hall effect (SHE; ref. 61). Right panel: BLS spectra of the thermal spin-wave fluctuations at electric currents below the onset of the auto-oscillation. The spin-current-induced auto-oscillation peak is marked with a vertical arrow. **c**, Experimental layout for the STT-based control of spin-wave damping in magnetic dielectric YIG (ref. 62). The electric current is applied to the 7-nm-thick Pt layer on top of a 20-nm-thick YIG disk. Spin-wave spectra measured by magnetic resonance force microscopy (MRFM) are shown below for different currents. The linewidth of the mode of highest amplitude (shaded area) is used for the determination of the effective spin-wave damping.

temporal[36] and phase[32,71] information for a wide range of frequencies and wavenumbers.

Magnon excitation by spin-transfer torque

To combine magnonic devices with electronic circuits, efficient means for magnon excitation by a charge current are required. Although magnons can be injected relatively easily by an a.c. electric current (for example, using antenna structures), it is a fairly complex problem if a d.c. current is used. One of the most promising solutions is usage of the spin-transfer-torque (STT) effect. In 1996, Slonczewski[72] and Berger[73] predicted independently that the injection of a spin-polarized current in a magnetic metallic film can generate a spin-transfer torque strong enough to reorient the magnetization or to excite magnetization precession[74] in this film. To generate the spin-polarized current, the d.c. charge current is sent through an additional magnetic layer with a fixed magnetization direction. The device, especially designed to excite magnetization precession, is named a spin-torque nano-oscillator (STNO). The first microwave measurement of spin-torque-driven precession was presented in 1998 by Tsoi and colleagues[75]. Krivorotov *et al.* have demonstrated experimentally that STT can be used to control the magnetic damping and for magnetization reversal of a nanomagnet[76].

The excitation of spin waves by a STNO was observed by Demidov and colleagues[59]. The authors used BLS spectroscopy to perform a two-dimensional mapping of waves emitted by the STNO into an in-plane magnetized Permalloy film. It was reported that the emission is directional and depends on the orientation of the applied magnetic field. However, as the propagation length of the emitted waves did not exceed one micrometre, the propagating character of the waves was not proved. Another report on spin-wave generation by a STNO was presented by Madami and colleagues[60]. The authors used a normally magnetized Permalloy film, which was probed by BLS spectroscopy—see Fig. 2a. In this case, the radial emission of spin waves propagating over a distance of a few micrometres was observed (see Fig. 2a). The magnon free path obtained from the data presented in Fig. 2a agrees well with a theoretical estimation.

A different way to generate a spin-polarized electron current is based on the spin Hall effect (SHE) caused by spin-dependent scattering of electrons in a non-magnetic metal or semiconductor with large spin–orbit interaction[77,78]. Electrons flowing in a film, magnetized in-plane and transversely to the current direction, scatter with spin-asymmetry, generating a spin current perpendicular to the film plane. This current, crossing the interface to an attached magnetic layer, generates a STT in this layer. A typical metal used in SHE studies is Pt (refs 79,80). Its thickness varies between 2 and 10 nm: these values are close to the spin-diffusion length in Pt (refs 81–83).

A great advantage of the SHE as a spin-current source is that a STT can be injected not only into a single local object (the diameter of a typical STNO is less than 100 nm) but into a large area of a magnetic film. That allows the realization of spin-wave amplification via damping compensation. The first experimental observation of SHE-induced damping reduction was reported by Ando *et al.*[79] in a Py/Pt bilayer. In follow-up studies[80], the variation of the damping parameter by a factor of four was demonstrated in Py/Cu/Pt multilayers studied by means of BLS spectroscopy. However, no spin-wave generation was achieved in these experiments, the probable reason being the strong nonlinear redistribution of the injected energy between many magnon modes. In subsequent studies, a modified design of the current-conducting structure, containing bowtie-shaped electrodes with a 100 nm gap in between (see Fig. 2b), was used[61]. These electrodes allow an increase in the density of the electric current applied to the Pt layer[62] and the introduction of a controlled radiation loss mechanism for the parasitic magnon modes previously disturbing the generation process. Consequently, the injected energy was concentrated into the small area between the electrodes, and a single bullet-like spatially localized magnon mode was observed. The coherency of this mode was proven by Liu *et al.* in microwave measurements[84]. Recently, Duan *et al.*[85] demonstrated microwave oscillations of the magnetization in a ferromagnetic nanowire, where the geometric confinement dilutes the magnon spectrum and, thus, suppresses the parasitic nonlinear energy redistribution.

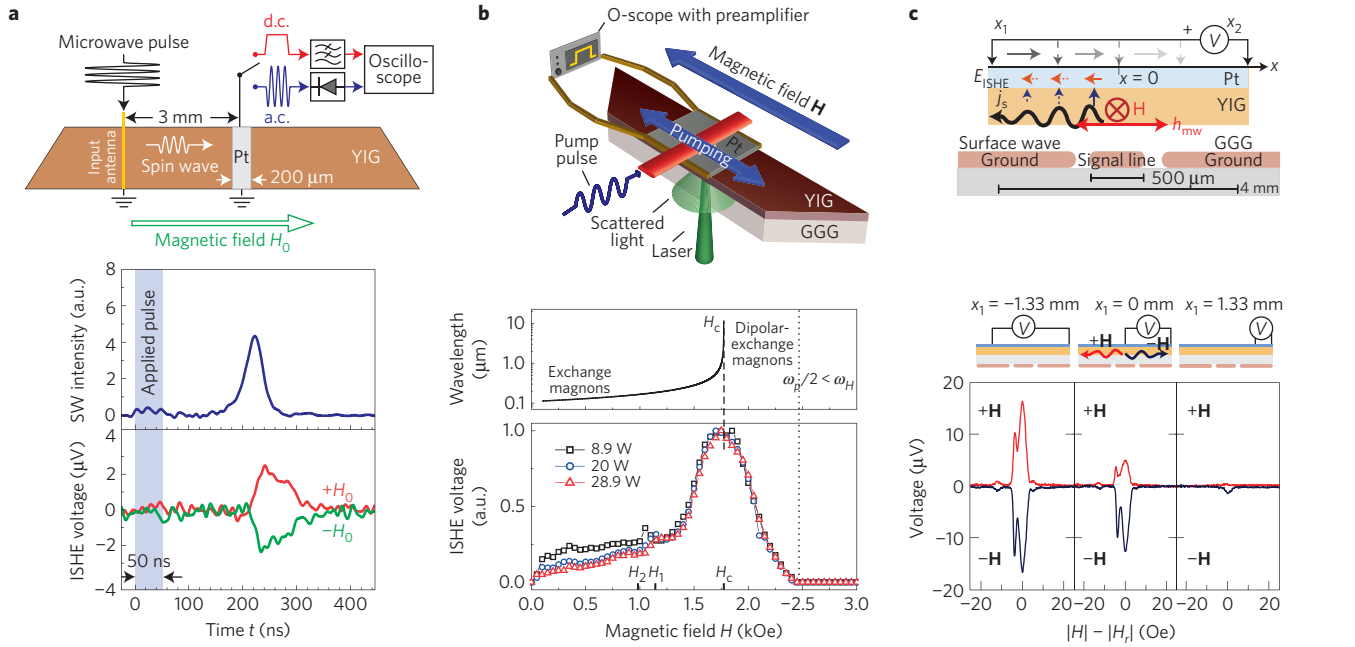

Figure 3 | Conversion of magnons into charge currents. a, Experimental set-up for the inverse spin Hall effect (ISHE) detection of propagating spin waves[70]. A spin-wave packet is excited in the YIG conduit using a microstrip antenna and is detected by the Pt strip as a.c. and d.c. signals. Temporal evolutions of the spin-wave intensity (a.c. signal) and the ISHE voltage (d.c. signal) are shown in the bottom panel for different field polarities. **b**, Experimental set-up for the investigation of spin pumping by parametrically injected exchange magnons[69]. A 10-nm-thick, 3×3 mm^2 Pt layer is deposited onto the 2.1-μm-thick YIG film. Middle panel: Calculated wavelength of the parametrically injected magnons. Bottom panel: Normalized dependencies of the ISHE voltage as a function of the bias magnetic field for different pump powers. **c**, Set-up for studies of spin pumping by nonreciprocal spin waves (adapted from ref. 108). Two needle probes contacting the surface of the Pt layer are connected to a voltmeter. Bottom panel: Voltage measured as a function of bias magnetic field at different probe positions (see sketches) for different magnetic field polarities.

Another important advantage of the SHE-based STT is that no electric current flows across the magnetic layer and, thus, the usage of a low-damping magnetic dielectric material such as YIG is possible. In the pioneering work of Kajiwara *et al.*[86] the transmission of a d.c. electric signal through a YIG film was demonstrated. For that, the SHE-based STT was used to convert a d.c. current into travelling spin waves. However, the exact conditions required for such conversion[53,87,88], or even for the SHE-STT-based damping compensation[89,90], were not defined. In this context, special attention has been attracted by recent work of Hamadeh *et al.* where bowtie-like electrodes (see Fig. 2c) were used for the damping compensation in YIG discs[62]. The decrease of the ferromagnetic resonance linewidth (which is a measure of the magnetic damping) by a factor of three was reported.

It was also demonstrated that a spin current and, consequently, the STT may be induced by a thermal gradient rather than by an electric current and the SHE effect[91–93]. This approach opens the door for the effective conversion of waste heat into electrical voltages or even spin waves for further data transfer and processing[65,71,94–97].

Conversion of magnon currents into electron currents

The structure of magnon spintronics as shown in Fig. 1 assumes that after information is processed within a magnonic system it needs to be converted back to electronic signals. A conventional way to do this is to use a strip antenna or a coplanar antenna, in which spin waves induce an a.c. current that, by turn, is rectified by a semiconductor diode[22]. Another recently discovered way is based on the combination of two physical effects: spin pumping (SP) and the inverse spin Hall effect (ISHE). In 2002, Tserkovnyak *et al.*[67] showed theoretically that magnetization precession in a magnetic film will generate a spin-polarized electric current in an attached non-magnetic metallic layer. This process manifests itself in the increase in damping of a magnonic system[67,98,99]. Electrical detection of the spin-pumping-induced spin current was reported by Costache and colleagues[100]. In the same year, Saitoh *et al.*[68] reported the observation of spin pumping using the ISHE. This effect refers to the generation of a charge current in a non-magnetic metal by a spin current. Owing to this effect, a spin current induced in a Pt film by a precessing magnetization in an adjacent magnetic film is converted into a d.c. voltage. Since then, a combined SP-ISHE mechanism has been used as a convenient detection mechanism for magnons (see, for example, the review by Hoffman[82]).

The SP-ISHE mechanism allows measurements of the magnetization precession not only in metallic-based but also in YIG-based structures. A first report of Kajiwara *et al.* on the observation of an ISHE voltage in YIG/Pt bilayers[86] was followed by comprehensive studies of this phenomenon: The dependencies on the thicknesses of the non-magnetic metal[81,87,96] and the YIG (refs 101,102) layer, as well as on the applied microwave power[102] have been reported. The influence of the interface conditions on the spin-pumping efficiency[103,104] was revealed, and the contributions to the SP effect by different spin-wave modes were studied[88,105].

An important milestone was the successful implementation of the combined SP-ISHE mechanism for the detection of propagating spin waves[70]. A typical geometry is shown in Fig. 3a. A spin-wave detector in the form of a 200-μm-wide Pt strip was placed 3 mm away from the microstrip antenna. The Pt strip was used for the detection of the ISHE voltage, as well as, for reference, as a conventional inductive probe. In the bottom panels of Fig. 3a, both the a.c. and the d.c. signals produced by a 50-ns-long spin-wave pulse are shown. One can clearly see that the ISHE voltage appears with a delay of 200 ns determined by the spin-wave propagation time between the antenna and the detector. The ISHE nature of the d.c. signal is evidenced by the fact that the inversion of the direction of a biasing magnetic field results in a switching of

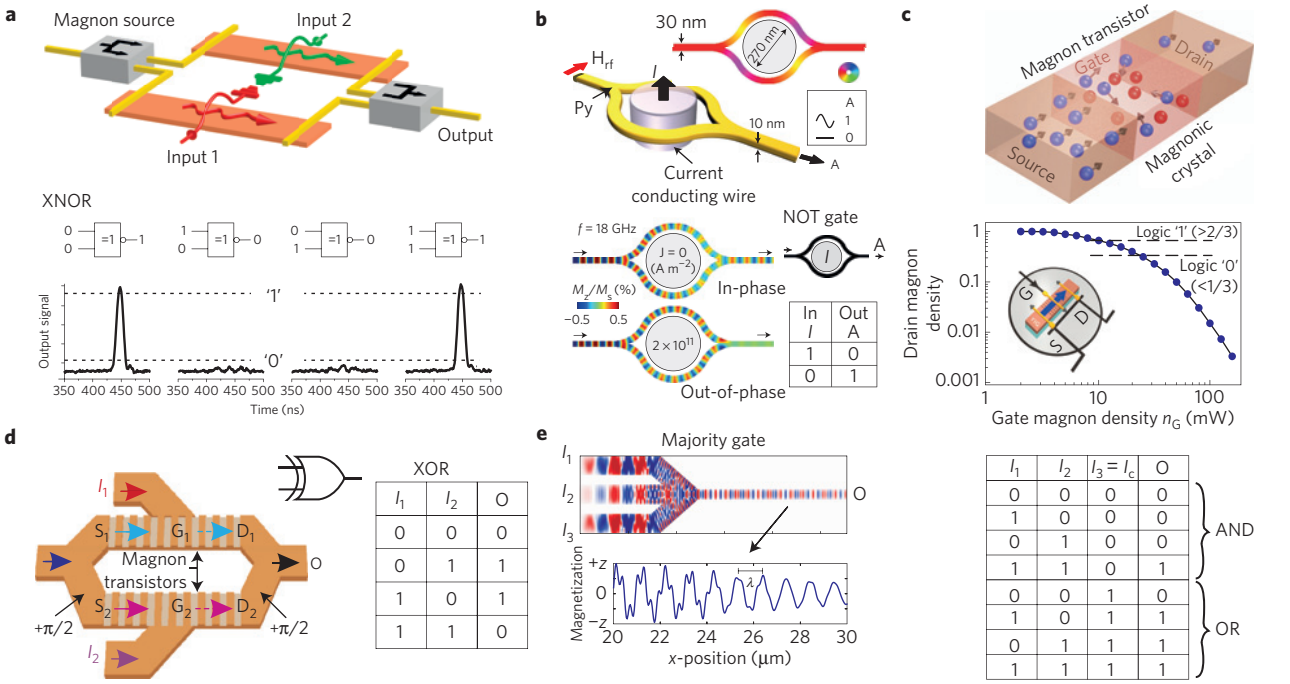

In I	Out A
1	0
0	1

I_1	I_2	O
0	0	0
0	1	1
1	0	1
1	1	0

I_1	I_2	$I_3 = I_c$	O	
0	0	0	0	AND
1	0	0	0	
0	1	0	0	
1	1	0	1	
0	0	1	0	OR
1	0	1	1	
0	1	1	1	
1	1	1	1	

Figure 4 | Magnon-based processing of binary data. **a**, Spin-wave XNOR logic gate based on a Mach–Zehnder interferometer with electric current-controlled phase shifters[10,47]. The bottom panel shows the output pulsed spin-wave signals measured for different combinations of the input d.c. signals. **b**, Nanosized Mach–Zehnder spin-wave interferometer designed in the form of a bifurcated Py conduit girdling a vertical conducting wire (adapted from ref. 11). The simulation of a NOT logic operation is shown below for two different d.c. currents, which correspond to the logic '0' and '1' inputs, respectively. **c**, Operational principle of a magnon transistor[7]: the source-to-drain magnon current (blue spheres) is nonlinearly scattered by gate magnons (red spheres) injected into the gate region. The spatial localization and, as a consequence, a high density of the gate magnons is provided by a magnonic crystal. The measured drain magnon density is presented in the bottom panel. **d**, All-magnon chip proposed for XOR logic operation. The magnon densities sent to the transistor sources S_1 and S_2 are controlled by the input magnon signals I_1 and I_2 applied to the gates zG_1 and G_2. In the case when both input signals are '0', the output signal is also '0' owing to destructive interference. The application of the magnon signal to only one of the gates switches off one of the source-to-drain currents and results in the '1' output. Finally, switching off both currents results in the output '0'—see the truth table. **e**, Majority gate operating with data coded into the spin-wave phase[17]. The colour map represents the spin-wave amplitude for the case of equal input phases. The majority gate can perform OR and AND logic operations (also NOR and NAND if the read-out position is shifted by $\lambda/2$) if one of its inputs is used as a control input I_C—see the truth table.

the voltage polarity[106]—see the figure. In the same experiment, it was also demonstrated that the spin-pumping efficiency does not depend on the spin-wave wavelength[70]. d'Allivy Kelly *et al.* have used a similar experimental set-up to demonstrate the ISHE detection of propagating magnons in a nanometre-thick YIG film[53].

Recently, the combined SP-ISHE mechanism has opened doors for access to short-wavelength exchange magnons[69]. The short-wavelength regime is of particular interest for nanosize magnonic applications. To excite exchange magnons, a parallel parametric pumping technique can be used[22,57,69]—see Fig. 3b. By variation of the bias magnetic field, the magnon spectrum is shifted up or down to tune the magnon wavelength (see inner panel in Fig. 3b). The spin-pumping-induced ISHE voltage is shown in the bottom panel of Fig. 3b. One can see that magnons effectively contribute to the spin pumping in a wide range of wavelengths (down to 100 nm in ref. 69). Follow-up studies by Kurebayashi *et al.*[107], where parallel and perpendicular parametric pumping techniques were used for the magnon injection, have evidenced that the spin-pumping efficiency is independent of the magnon wavelength within experimental error.

Magnetostatic surface spin waves show nonreciprocal behaviour (see Box 1). The propagation direction of these waves can be reversed by a change in the polarity of the bias magnetic field[30]. As a result, the ISHE voltage induced by the MSSWs depends on the field orientation[108]. Results of experimental studies where an electric probe was used to measure the ISHE voltage at different points of a sample are shown in Fig. 3c.

To summarize, the combined SP-ISHE mechanism allows simple conversion of magnon currents into charge currents. It was demonstrated that magnons, independently of their nature (exchange or dipolar) and characteristics (wavelengths, frequencies, velocities, and so on), efficiently contribute to spin pumping. Moreover, the SP-ISHE detection technique is of crucial importance for the miniaturization of magnonic devices as it is sensitive to magnons of very small wavelengths that cannot be detected by microwave and optical methods[69]. The conversion efficiency is large enough for the realization of first demonstrators, but needs to be improved for device applications.

Magnon-based data processing

In the previous sections, we discussed interconnections between magnon-based units and electronic circuits. However, the main strength of magnon spintronics lies in the benefits provided by the wave nature of magnons for data processing and computation. In the past, the application area of spin waves was mostly related to analogue signal processing in the microwave frequency range. Microwave filters, delay lines, phase conjugators, power limiters and amplifiers are just a few examples[5,6]. Nowadays, new technologies, allowing, for example, the fabrication of nanometre-sized structures or operation in the THz frequency range, in combination with novel physical phenomena, provide new momentum to the field and make

Box 2 | Artificial magnetic materials—magnonic crystals—for data transfer and processing.

Magnonic crystals are artificial magnetic media with a periodic variation of their magnetic properties in space. Bragg scattering affects the spin-wave spectrum of such a structure. This leads to the formation of bandgaps—regions of the spin-wave spectrum in which spin-wave propagation is prohibited (see right panels in Fig. B1a and b). Consequently, areas between bandgaps allow selective spin-wave propagation[22,46,110,111], whereas the pronounced changes of the spin-wave dispersion near the bandgap edges open access to the formation of bandgap solitons[115], deceleration of spin waves and the appearance of confined spin-wave modes[37].

The wide variety of parameters, which define the characteristics of spin waves in a magnetic film, results in a variety of possible designs of magnonic crystals[111]. For example, magnonic crystals can be constructed using two different magnetic materials (bi-component magnonic crystals[116])—see Fig. B1a. Other examples are spin-wave conduits with periodic variations of their width (Fig. B1b)[117], thickness[22,118], saturation magnetization[119], periodic dot or anti-dot lattices[46,51,120], and arrays of interacting magnetic strips (Fig. B1c)[110,111].

Initially, periodic magnetic structures were used as Bragg mirrors in microwave filters, resonators and generators[121]. Nowadays, the interest for magnonic crystals is much broader. In particular, magnonic crystals are used for guiding spin waves[46,111], as generators[122], magnetic field sensors[123], power limiters[39], and for short-time data buffers[37,124].

Reconfigurable magnonic crystals, whose properties can be changed on demand[111,112], attract special attention. Figure B1c represents a magnonic crystal in the form of an array of parallel- or anti-parallel-magnetized magnetic strips. The chosen magnetization state defines the lattice constant of the crystal and, thus, the spin-wave dispersion (see right panel). Very recently, we have demonstrated that any 2D magnetization pattern in a magnetic film can be reconfigurably created by laser-induced heating[125].

Change in the properties of a crystal open access to novel physics if these changes occur on a timescale shorter than the spin-wave propagation time across the crystal (dynamic magnonic crystal). The first dynamic magnonic crystal was realized in the form of a YIG conduit placed in a time-dependent spatially periodic magnetic field. The field was induced by a pulsed d.c. current sent through a meander-type conducting structure placed nearby the conduit surface and could be changed on a timescale below 10 ns (ref. 113). It has been shown that this dynamic magnonic crystal can perform a set of spectral transformations such as frequency inversion and time reversal[126]. The right panel of Fig. B1d demonstrates that frequencies of the spin wave reflected from the dynamic crystal are inverted relative to the frequencies of the input waves. Recently, Nikitin *et al.*[114] created a dynamic magnonic crystal on the base of a width-modulated YIG strip and used it for the realization of logic operations.

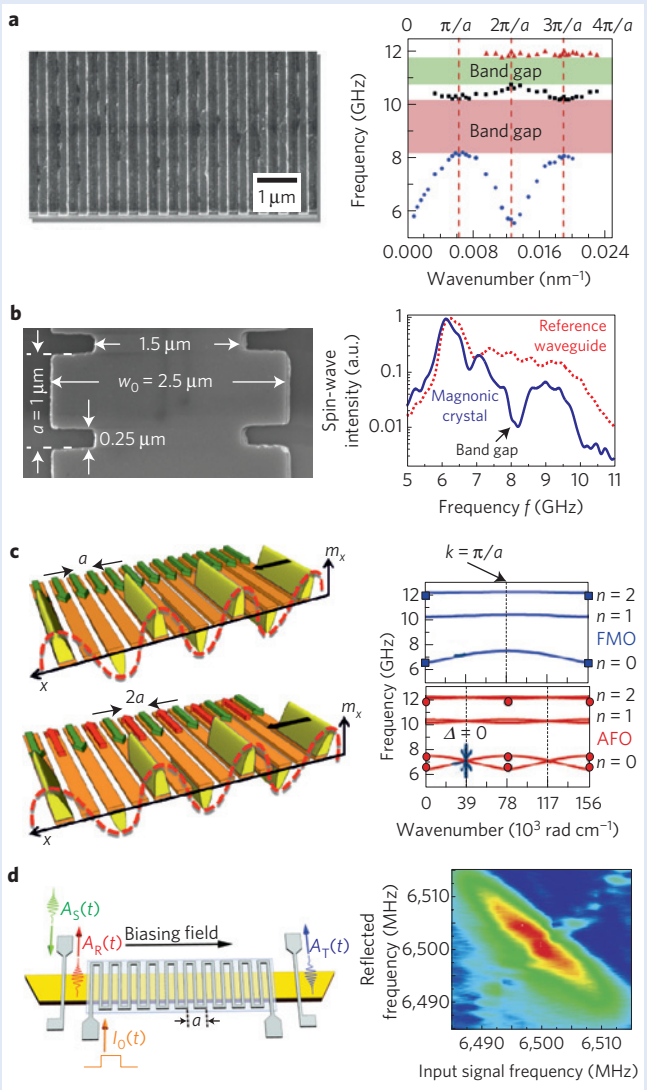

Figure B1 | Realizations of magnonic crystals. a, One-dimensional magnonic crystal in the form of an array of alternating Py and Co nanostripes and the structure of magnon bandgaps measured by BLS spectroscopy[116]. **b**, Magnonic crystal designed as a Py conduit with a periodically varying width, and spin-wave spectra of this crystal and of a uniform reference conduit[117]. **c**, Reconfigurable magnonic crystal in the form of an array of bi-stable magnetic nanowires and spin-wave spectra obtained for ferromagnetic and antiferromagnetic nanowires orders[111,112]. **d**, Schematics of a dynamic magnonic crystal in the form of a current-carrying meander structure positioned close to the surface of a YIG conduit[126]. A two-dimensional map of the reflected signal spectra as a function of the incident signal frequency is shown on the right.

the advantages discussed in Box 1 accessible for both analogue and digital data processing.

In this respect, artificial magnetic materials with properties periodically varied in space, known as magnonic crystals[109], are especially promising for controlling and manipulating the magnon currents—see Box 2. Similarly to photonic crystals operated with light, magnonic crystals use the wave nature of magnons to obtain magnon propagation characteristics that are inaccessible by any other means (see reviews[22,46,110,111]). This allows one to combine one- and two-dimensional magnon waveguiding with magnon-based data processing. Furthermore, reconfigurable[111,112,125] and dynamic magnonic crystals[113,114] demonstrate potential for the realization of universal data processing units, which can perform different data operations on demand (see Box 2)[115–126].

Magnons have potential for the implementation of alternative computing concepts such as non-Boolean computing[14,15], reversible logic overcoming the Landauer limit of energy consumption[18,19], artificial neural networks[127], and, more general, projecting optical computing concepts[9] onto the nanometre scale; these directions are still in the early stages of their development. As an introduction

to these developments we address standard logic operations with digital binary data that are at present the subject of intensive theoretical and experimental studies. The idea of encoding binary data into the spin-wave amplitude was first stated by Kostylev and colleagues[128]. It was proposed to use a Mach–Zehnder spin-wave interferometer equipped with current-controlled phase shifters embedded in the interferometer arms to construct logic gates. Following this idea, Schneider *et al.* realized the proof-of-principle XNOR logic gate shown in Fig. 4a[10]. The currents applied to Input 1 and Input 2 represent logic inputs: the current-on state, which results in a π-phase shift of the spin wave in the respective interferometer arm, corresponds to logic '1'; the current-off state corresponds to logic '0'. The logic output is defined by the interference of microwave currents induced by the spin waves in the output microstrip antennas: a small amplitude level (destructive interference) corresponds to logic '0', and a high amplitude level (constructive interference) defines logic '1'. The change in the magnitude of the output pulsed signal for different combinations of the logic inputs (see Fig. 4a) corresponds to the XNOR logic functionality[10]. It was also shown that an electric current can create a magnetic barrier, reducing or even stopping the spin-wave transmission. Using this effect a universal NAND logic gate was realized[10].

Lee *et al.*[11] have proposed an alternative design of a nanometre-sized logic gate—see Fig. 4b. In this device, the spin-wave phases are controlled via a d.c. current flowing through a vertical wire placed between the interferometer arms. This d.c. current defines the logic input, whereas the amplitude of the output spin wave defines the logic output. The ability to create NOT, NOR and NAND logic gates was demonstrated using numerical simulations.

The drawback of the discussed logic gates is that it is impossible to combine two logic gates without additional magnon-to-voltage and voltage-to-magnon converters. This fact, in combination with relatively weak efficiencies of the existing converters, stimulates the search for a means to control a magnon current by another magnon current. Recently, it has been demonstrated that such control is possible owing to nonlinear magnon–magnon scattering, and a magnon transistor allowing all-magnon data processing has been realized[7]—see Fig. 4c. In this three-terminal device, the density of the magnon current flowing from the source to the drain (see blue spheres in the figure) is controlled by the magnons injected into the gate of the transistor (red spheres). The magnonic crystal in the form of an array of surface grooves[118] is used to increase the density of the gate magnons and, consequently, to enhance the efficiency of the nonlinear four-magnon scattering process used to suppress the source-to-drain magnon current. It was shown that the source-to-drain magnon current can be decreased by up to three orders of magnitude (see bottom panel in Fig. 4c). The potential for miniaturization of this transistor as well as for an increase of its operating speed and a decrease in its energy consumption is discussed in ref. 7. Moreover, the magnon transistor can be used in forthcoming magnonic chips. For example, Fig. 4d represents an XOR gate in the form of a spin-wave interferometer with two magnon transistors embedded into its arms. This chip does not comprise any external antennas, it is planar, consists of only one material, and its output can be directly connected to the input of the next logic gate[7]. Moreover, this simple chip substitutes eight CMOS transistors and allows a reduction in the footprint of logic circuitry.

Alternatively, Khitun *et al.* proposed digitizing information using the spin-wave phase instead of the amplitude (see review[12]). Such an approach allows trivial embedding of a NOT logic element in magnonic circuits by changing the position of a read-out device by a distance $\lambda/2$. Moreover, it opens access to the realization of a majority logic gate in the form of a multi-input spin-wave combiner—see Fig. 4e. Klingler *et al.* proposed a fully functional design of a micro-structured spin-wave majority gate and tested it by micro-magnetic simulations[17]. It was shown that the same majority gate can perform AND, OR, NAND and NOR logic operations if one of its three inputs serves as a control input. The majority gate (similar to the magnon transistor) is suitable for the construction of all-magnon chips and allows a substantial decrease of the device footprint[12,15–17]. For example, to build a full adder, one needs only three majority gates instead of 28 transistors in CMOS. The majority gate operates with linear spin waves having amplitudes down to the thermal level and, thus, can reach an extremely low energy consumption down to 10^{-20} J per bit (estimated for a single bit carried by a 5-ns-long spin-wave packet).

Outlook

Despite recent advances, the field of magnon spintronics has many challenges remaining, both in physical and technological aspects[47]. Most of the advantages discussed in Box 1, including sub-100 nm and low-THz magnonics, are just behind the current level of realization, but should be within reach in the next few years. However, it is not possible to predict which of the research directions will be the most successful. All of them aim for low-energy means of magnon excitation, manipulation and detection on the nanometre scale, which, by turn, will have great potential for computing applications. New low-loss magnetic materials, which will allow a decrease in the energy consumption of magnonic devices, are of high priority; as are novel means for damping compensation, which will enable long-distance magnonic currents to be realized. Furthermore, recent discoveries have given rise to new sub-fields of magnonics. Only the very first steps have been made so far towards the utilization of heat-assisted effects in magnon spintronics such as the spin Seebeck effect[95]. To name a few others, Dzyaloshinskii–Moriya interactions[129–132], micro- and macroscopic quantum effects[42,44,131,132], and low-energy control and excitation of magnons with electric fields[133,134] are also subjects of accelerating research. The development of alternative concepts for post-CMOS computing, as well as the combination of magnon computing with data storage[135] look promising. The interactions of spin waves with domain walls[136] and skyrmions[137,138] attracting much interest in this context. Magnon spintronics is therefore an active, emergent field that could deliver a number of breakthrough developments towards application in data processing in the near future.

Received 18 January 2015; accepted 21 April 2015; published online 2 June 2015

References

1. Bloch, F. Zur Theorie des Ferromagnetismus. *Z. Phys.* **61,** 206–219 (1930).
2. Gurevich, A. G. & Melkov, G. A. *Magnetization Oscillations and Waves* (CRC, 1996).
3. Stancil, D. D. & Prabhakar, A. *Spin Waves: Theory and Applications* (Springer, 2009).
4. L'vov, V. S. *Wave Turbulence Under Parametric Excitation* (Springer, 1994).
5. Owens, J. M., Collins, J. H. & Carter, R. L. System applications of magnetostatic wave devices. *Circuits Syst. Signal Process.* **4,** 317–334 (1985).
6. Adam, J. D. Analog signal processing with microwave magnetics. *Proc. IEEE* **76,** 159–170 (1988).
7. Chumak, A. V., Serga, A. A. & Hillebrands, B. Magnon transistor for all-magnon data processing. *Nature Commun.* **5,** 4700 (2014).
8. Vogt, K. *et al.* Realization of a spin-wave multiplexer. *Nature Commun.* **5,** 3727 (2014).
9. Feitelson, D. C. *Optical Computing: A Survey for Computer Scientists* (MIT Press, 1992).
10. Schneider, T. *et al.* Realization of spin-wave logic gates. *Appl. Phys. Lett.* **92,** 022505 (2008).
11. Lee, K-S. & Kim, S-K. Conceptual design of spin wave logic gates based on a Mach–Zehnder-type spin wave interferometer for universal logic functions. *J. Appl. Phys.* **104,** 053909 (2008).
12. Khitun, A., Bao, M. & Wang, K. L. Magnonic logic circuits. *J. Phys. D* **43,** 264005 (2010).
13. Sato, N., Sekiguchi, K. & Nozaki, Y. Electrical demonstration of spin-wave logic operation. *Appl. Phys. Express* **6,** 063001 (2013).

14. Csaba, G., Papp, A. & Porod, W. Spin-wave based realization of optical computing primitives. *J. Appl. Phys.* **115,** 17C741 (2014).
15. Khasanvis, S., Rahman, M., Rajapandian, S. N. & Moritz, C. A. *IEEE/ACM Int. Symp. Nanoscale Archit.* (*NANOARCH*) 171–176 (IEEE, 2014).
16. Khitun, A. & Wang, K. L. Non-volatile magnonic logic circuits engineering. *J. Appl. Phys.* **110,** 034306 (2011).
17. Klingler, S. *et al.* Design of a spin-wave majority gate employing mode selection. *Appl. Phys. Lett.* **105,** 152410 (2014).
18. Bérut, A. *et al.* Experimental verification of Landauer's principle linking information and thermodynamics. *Nature* **483,** 187–189 (2012).
19. Cuykendall, R. & Andersen, D. R. Reversible optical computing circuits. *Opt. Lett.* **12,** 542–544 (1987).
20. Khitun, A. Multi-frequency magnonic logic circuits for parallel data processing. *J. Appl. Phys.* **111,** 054307 (2012).
21. Cherepanov, V., Kolokolov, I. & L'vov, V. The saga of YIG: Spectra, thermodynamics, interaction and relaxation of magnons in a complex magnet. *Phys. Rep.* **229,** 81–144 (1993).
22. Serga, A. A., Chumak, A. V. & Hillebrands, B. YIG magnonics. *J. Phys. D* **43,** 264002 (2010).
23. Balashov, T., Buczek, P., Sandratskii, L., Ernst, A. & Wulfhekel, W. Magnon dispersion in thin magnetic films. *J. Phys. Condens. Matter* **26,** 394007 (2014).
24. Chuang, T-H. *et al.* Magnetic properties and magnon excitations in Fe(001) films grown on Ir(001). *Phys. Rev. B* **89,** 174404 (2014).
25. Pirro, P. *et al.* Spin-wave excitation and propagation in microstructured waveguides of yttrium iron garnet/Pt bilayers. *Appl. Phys. Lett.* **104,** 012402 (2014).
26. Hahn, C. *et al.* Measurement of the intrinsic damping constant in individual nanodisks of $Y_3Fe_5O_{12}$ and $Y_3Fe_5O_{12}$|Pt. *Appl. Phys. Lett.* **104,** 152410 (2014).
27. Au, Y. *et al.* Resonant microwave-to-spin-wave transducer. *Appl. Phys. Lett.* **100,** 182404 (2012).
28. Verba, R. *et al.* Conditions for the spin wave nonreciprocity in an array of dipolarly coupled magnetic nanopillars. *Appl. Phys. Lett.* **103,** 082407 (2013).
29. Jamali, M., Kwon, J. H., Seo, S. M., Lee, K. J. & Yang, H. Spin wave nonreciprocity for logic device applications. *Sci. Rep.* **3,** 3160 (2013).
30. Schneider, T., Serga, A. A., Neumann, T., Hillebrands, B. & Kostylev, M. P. Phase reciprocity of spin-wave excitation by a microstrip antenna. *Phys. Rev. B* **77,** 214411 (2008).
31. Demidov, V. E. *et al.* Excitation of microwaveguide modes by a stripe antenna. *Appl. Phys. Lett.* **95,** 112509 (2009).
32. Demidov, V. E. *et al.* Excitation of short-wavelength spin waves in magnonic waveguides. *Appl. Phys. Lett.* **99,** 082507 (2011).
33. Schneider, T. *et al.* Nondiffractive subwavelength wave beams in a medium with externally controlled anisotropy. *Phys. Rev. Lett.* **104,** 197203 (2010).
34. Gieniusz, R. *et al.* Single antidot as a passive way to create caustic spin-wave beams in yttrium iron garnet films. *Appl. Phys. Lett.* **102,** 102409 (2013).
35. Kalinikos, B. A., Kovshikov, N. G. & Slavin, A. N. Experimental observation of magnetostatic wave envelope solitons in yttrium iron garnet films. *Phys. Rev. B* **42,** 8658–8660 (1990).
36. Serga, A. A. *et al.* Parametric generation of forward and phase-conjugated spin-wave bullets in magnetic films. *Phys. Rev. Lett.* **94,** 167202 (2005).
37. Chumak, A. V. *et al.* Storage-recovery phenomenon in magnonic crystal. *Phys. Rev. Lett.* **108,** 257207 (2012).
38. Melkov, G. A., Serga, A. A., Tiberkevich, V. S., Oliynyk, A. N. & Slavin, A. N. Wave front reversal of a dipolar spin wave pulse in a nonstationary three-wave parametric interaction. *Phys. Rev. Lett.* **84,** 3438–3441 (2000).
39. Ustinov, A. B., Drozdovskii, A. V. & Kalinikos, B. A. Multifunctional nonlinear magnonic devices for microwave signal processing. *Appl. Phys. Lett.* **96,** 142513 (2010).
40. Demokritov, S. O. *et al.* Bose–Einstein condensation of quasi-equilibrium magnons at room temperature under pumping. *Nature* **443,** 430–433 (2006).
41. Serga, A. A. *et al.* Bose–Einstein condensation in an ultra-hot gas of pumped magnons. *Nature Commun.* **5,** 3452 (2014).
42. Takei, S. & Tserkovnyak, Y. Superfluid spin transport through easy-plane ferromagnetic insulators. *Phys. Rev. Lett.* **112,** 227201 (2014).
43. Troncosoa, R. E. & Núñez, A. S. Josephson effects in a Bose–Einstein condensate of magnons. *Ann. Phys.* **346,** 182–194 (2014).
44. Nakata, K., van Hoogdalem, K. A., Simon, P. & Loss, D. Josephson and persistent spin currents in Bose–Einstein condensates of magnons. *Phys. Rev. B* **90,** 144419 (2014).
45. Kruglyak, V. V., Demokritov, S. O. & Grundler, D. Magnonics. *J. Phys. D* **43,** 264001 (2010).
46. Lenk, B., Ulrichs, H., Garbs, F. & Münzenberg, M. The building blocks of magnonics. *Phys. Rep.* **507,** 107–136 (2011).
47. Stamps, R. L. *et al.* The 2014 Magnetism Roadmap. *J. Phys. D* **47,** 333001 (2014).
48. Kalinikos, B. A. & Slavin, A. N. Theory of dipole-exchange spin-wave spectrum for ferromagnetic films with mixed exchange boundary conditions. *J. Phys. C* **19,** 7013–7033 (1986).
49. Kubota, T. *et al.* Half-metallicity and Gilbert damping constant in $Co_2Fe_xMn_{1-x}Si$ Heusler alloys depending on the film composition. *Appl. Phys. Lett.* **94,** 122504 (2009).
50. Sebastian, T. *et al.* Low-damping spin-wave propagation in a micro-structured $Co_2Mn_{0.6}Fe_{0.4}Si$ Heusler waveguide. *Appl. Phys. Lett.* **100,** 112402 (2012).
51. Ulrichs, H., Lenk, B. & Münzenberg, M. Magnonic spin-wave modes in CoFeB antidot lattices. *Appl. Phys. Lett.* **97,** 092506 (2010).
52. Conca, A. *et al.* Annealing influence on the Gilbert damping parameter and the exchange constant of CoFeB thin films. *Appl. Phys. Lett.* **104,** 182407 (2014).
53. d'Allivy Kelly, O. *et al.* Inverse spin Hall effect in nanometer-thick yttrium iron garnet/Pt system. *Appl. Phys. Lett.* **103,** 082408 (2013).
54. Onbasli, M. C. *et al.* Pulsed laser deposition of epitaxial yttrium iron garnet films with low Gilbert damping and bulk-like magnetization. *APL Mater.* **2,** 106102 (2014).
55. Liu, T. *et al.* Ferromagnetic resonance of sputtered yttrium iron garnet nanometer films. *J. Appl. Phys.* **115,** 17A501 (2014).
56. Vlaminck, V. & Bailleul, M. Current-induced spin-wave Doppler shift. *Science* **322,** 410–413 (2008).
57. Brächer, T. *et al.* Time- and power-dependent operation of a parametric spin-wave amplifier. *Appl. Phys. Lett.* **105,** 232409 (2014).
58. Dutta, S., Nikonov, D. E., Manipatruni, S., Young, I. A. & Naeemi, A. SPICE circuit modeling of PMA spin wave bus excited using magnetoelectric effect. *IEEE Trans. Magn.* **50,** 1300411 (2014).
59. Demidov, V. E., Urazhdin, S. & Demokritov, S. O. Direct observation and mapping of spin waves emitted by spin-torque nano-oscillators. *Nature Mater.* **9,** 984–988 (2010).
60. Madami, M. *et al.* Direct observation of a propagating spin wave induced by spin-transfer torque. *Nature Nanotech.* **6,** 635–638 (2011).
61. Demidov, V. E. *et al.* Magnetic nano-oscillator driven by pure spin current. *Nature Mater.* **11,** 1028–1031 (2012).
62. Hamadeh, A. *et al.* Full control of the spin-wave damping in a magnetic insulator using spin–orbit torque. *Phys. Rev. Lett.* **113,** 197203 (2014).
63. Bauer, H. G., Chauleau, J-Y., Woltersdorf, G. & Back, C. H. Coupling of spinwave modes in wire structures. *Appl. Phys. Lett.* **104,** 102404 (2014).
64. Demokritov, S. O., Hillebrands, B. & Slavin, A. N. Brillouin light scattering studies of confined spin waves: Linear and nonlinear confinement. *Phys. Rep.* **348,** 441–489 (2001).
65. An, T. *et al.* Unidirectional spin-wave heat conveyer. *Nature Mater.* **12,** 549–553 (2013).
66. Schultheiss, H., Pearson, J. E., Bader, S. D. & Hoffmann, A. Thermoelectric detection of spin waves. *Phys. Rev. Lett.* **109,** 237204 (2012).
67. Tserkovnyak, Y., Brataas, A. & Bauer, G. E. W. Enhanced Gilbert damping in thin ferromagnetic films. *Phys. Rev. Lett.* **88,** 117601 (2002).
68. Saitoh, E., Ueda, M., Miyajima, H. & Tatara, G. Conversion of spin current into charge current at room temperature: Inverse spin-Hall effect. *Appl. Phys. Lett.* **88,** 182509 (2006).
69. Sandweg, C. W. *et al.* Spin pumping by parametrically excited exchange magnons. *Phys. Rev. Lett.* **106,** 216601 (2011).
70. Chumak, A. V. *et al.* Direct detection of magnon spin transport by the inverse spin Hall effect. *Appl. Phys. Lett.* **100,** 082405 (2012).
71. Obry, B., Vasyuchka, V. I., Chumak, A. V., Serga, A. A. & Hillebrands, B. Spin-wave propagation and transformation in a thermal gradient. *Appl. Phys. Lett.* **101,** 192406 (2012).
72. Slonczewski, J. C. Current-driven excitation of magnetic multilayers. *J. Magn. Magn. Mater.* **159,** L1–L7 (1995).
73. Berger, L. Emission of spin waves by a magnetic multilayer traversed, by a current. *Phys. Rev. B* **54,** 9353–9358 (1996).
74. Slavin, A. & Tiberkevich, V. Nonlinear auto-oscillator theory of microwave generation by spin-polarized current. *IEEE Trans. Magn.* **45,** 1875–1918 (2009).
75. Tsoi, M. *et al.* Excitation of a magnetic multilayer by an electric current. *Phys. Rev. Lett.* **80,** 4281–4284 (1998).
76. Krivorotov, I. N. *et al.* Time-domain measurements of nanomagnet dynamics driven by spin-transfer torques. *Science* **307,** 228–231 (2005).
77. Dyakonov, M. I. & Perel, V. I. Current-induced spin orientation of electrons in semiconductors. *Phys. Lett. A* **35,** 459–460 (1971).
78. Hirsch, J. E. Spin Hall effect. *Phys. Rev. Lett.* **83,** 1834–1837 (1999).
79. Ando, K. *et al.* Electric manipulation of spin relaxation using the spin Hall effect. *Phys. Rev. Lett.* **101,** 036601 (2008).
80. Demidov, V. E., Urazhdin, S., Edwards, E. R. J. & Demokritov, S. O. Wide-range control of ferromagnetic resonance by spin Hall effect. *Appl. Phys. Lett.* **99,** 172501 (2011).

81. Castel, V., Vlietstra, N., Ben Youssef, J. & van Wees, B. J. Platinum thickness dependence of the inverse spin-Hall voltage from spin pumping in a hybrid yttrium iron garnet/platinum system. *Appl. Phys. Lett.* **101,** 132414 (2012).
82. Hoffmann, A. Spin Hall effects in metals. *IEEE Trans. Magn.* **49,** 5172–5193 (2013).
83. Ganguly, A. *et al.* Thickness dependence of spin torque ferromagnetic resonance in $Co_{75}Fe_{25}$/Pt bilayer films. *Appl. Phys. Lett.* **104,** 072405 (2014).
84. Liu, R. H., Lim, W. L. & Urazhdin, S. Spectral characteristics of the microwave emission by the spin Hall nano-oscillator. *Phys. Rev. Lett.* **110,** 147601 (2013).
85. Duan, Z. *et al.* Nanowire spin torque oscillator driven by spin orbit torques. *Nature Commun.* **5,** 5616 (2014).
86. Kajiwara, Y. *et al.* Transmission of electrical signals by spin-wave interconversion in a magnetic insulator. *Nature* **464,** 262–266 (2010).
87. Hahn, C. *et al.* Comparative measurements of inverse spin Hall effects and magnetoresistance in YIG/Pt and YIG/Ta. *Phys. Rev. B* **87,** 174417 (2013).
88. Xiao, J. & Bauer, G. E. W. Spin-wave excitation in magnetic insulators by spin-transfer torque. *Phys. Rev. Lett.* **108,** 217204 (2012).
89. Padron-Hernandez, E., Azevedo, A. & Rezende, S. M. Amplification of spin waves in yttrium iron garnet films through the spin Hall effect. *Appl. Phys. Lett.* **99,** 192511 (2011).
90. Wang, Z. H., Sun, Y. Y., Wu, M. Z., Tiberkevich, V. & Slavin, A. Control of spin waves in a thin film ferromagnetic insulator through interfacial spin scattering. *Phys. Rev. Lett.* **107,** 146602 (2011).
91. Padron-Hernandez, E., Azevedo, A. & Rezende, S. M. Amplification of spin waves by thermal spin-transfer torque. *Phys. Rev. Lett.* **107,** 197203 (2011).
92. Lu, L., Sun, Y. Y., Jantz, M. & Wu, M. Z. Control of ferromagnetic relaxation in magnetic thin films through thermally induced interfacial spin transfer. *Phys. Rev. Lett.* **108,** 257202 (2012).
93. Jungfleisch, M. B. *et al.* Heat-induced damping modification in yttrium iron garnet/platinum hetero-structures. *Appl. Phys. Lett.* **102,** 062417 (2013).
94. Uchida, K. *et al.* Spin Seebeck insulator. *Nature Mater.* **9,** 894–897 (2010).
95. Bauer, G. E. W., Saitoh, E. & van Wees, B. J. Spin caloritronics. *Nature Mater.* **11,** 391–399 (2012).
96. Weiler, M. *et al.* Experimental test of the spin mixing interface conductivity concept. *Phys. Rev. Lett.* **111,** 176601 (2013).
97. Agrawal, M. *et al.* Role of bulk-magnon transport in the temporal evolution of the longitudinal spin-Seebeck effect. *Phys. Rev. B* **89,** 224414 (2014).
98. Šimánek, E. & Heinrich, B. Gilbert damping in magnetic multilayers. *Phys. Rev. B* **67,** 144418 (2003).
99. Woltersdorf, G., Buess, M., Heinrich, B. & Back, C. H. Time resolved magnetization dynamics of ultrathin Fe(001) films: Spin-pumping and two-magnon scattering. *Phys. Rev. Lett.* **95,** 037401 (2005).
100. Costache, M. V., Sladkov, M., Watts, S. M., van der Wal, C. H. & van Wees, B. J. Electrical detection of spin pumping due to the precessing magnetization of a single ferromagnet. *Phys. Rev. Lett.* **97,** 216603 (2006).
101. Castel, V., Vlietstra, N., van Wees, B. J. & Ben Youssef, J. Yttrium iron garnet thickness and frequency dependence of the spin-charge current conversion in YIG/Pt systems. *Phys. Rev. B* **90,** 214434 (2014).
102. Jungfleisch, M. B. *et al.* Thickness and power dependence of the spin-pumping effect in $Y_3Fe_5O_{12}$/Pt heterostructures measured by the inverse spin Hall effect. *Phys. Rev. B* **91,** 134407 (2015).
103. Burrowes, C. *et al.* Enhanced spin pumping at yttrium iron garnet/Au interfaces. *Appl. Phys. Lett.* **100,** 092403 (2012).
104. Jungfleisch, M. B., Lauer, V., Neb, R., Chumak, A. V. & Hillebrands, B. Improvement of the yttrium iron garnet/platinum interface for spin pumping-based applications. *Appl. Phys. Lett.* **103,** 022411 (2013).
105. Kapelrud, A. & Brataas, A. Spin pumping and enhanced Gilbert damping in thin magnetic insulator films. *Phys. Rev. Lett.* **111,** 097602 (2013).
106. Schreier, M. *et al.* Sign of inverse spin Hall voltages generated by ferromagnetic resonance and temperature gradients in yttrium iron garnet platinum bilayers. *J. Phys. D* **48,** 025001 (2015).
107. Kurebayashi, H. *et al.* Spin pumping by parametrically excited short-wavelength spin waves. *Appl. Phys. Lett.* **99,** 162502 (2011).
108. Iguchi, R. *et al.* Spin pumping by nonreciprocal spin waves under local excitation. *Appl. Phys. Lett.* **102,** 022406 (2013).
109. Gulyaev, Y. V. *et al.* Ferromagnetic films with magnon bandgap periodic structures: Magnon crystals. *JETP Lett.* **77,** 567–570 (2003).
110. Gubbiotti, G. *et al.* Brillouin light scattering studies of planar metallic magnonic crystals. *J. Phys. D* **43,** 264003 (2010).
111. Krawczyk, M. & Grundler, D. Review and prospects of magnonic crystals and devices with reprogrammable band structure. *J. Phys. Condens. Matter* **26,** 123202 (2014).
112. Topp, J., Heitmann, D., Kostylev, M. P. & Grundler, D. Making a reconfigurable artificial crystal by ordering bistable magnetic nanowires. *Phys. Rev. Lett.* **104,** 207205 (2010).
113. Chumak, A. V., Neumann, T., Serga, A. A., Hillebrands, B. & Kostylev, M. P. A current-controlled, dynamic magnonic crystal. *J. Phys. D* **42,** 205005 (2009).
114. Nikitin, A. A. *et al.* A spin-wave logic gate based on a width-modulated dynamic magnonic crystal. *Appl. Phys. Lett.* **106,** 102405 (2015).
115. Drozdovskii, A. V., Cherkasskii, M. A., Ustinov, A. B., Kovshikov, N. G. & Kalinikos, B. A. Formation of envelope solitons of spin-wave packets propagating in thin-film magnon crystals. *JETP Lett.* **91,** 16–20 (2010).
116. Wang, Z. K. *et al.* Observation of frequency band gaps in a one-dimensional nanostructured magnonic crystal. *Appl. Phys. Lett.* **94,** 083112 (2009).
117. Chumak, A. V. *et al.* Spin-wave propagation in a microstructured magnonic crystal. *Appl. Phys. Lett.* **95,** 262508 (2009).
118. Chumak, A. V., Serga, A. A., Hillebrands, B. & Kostylev, M. P. Scattering of backward spin waves in a one-dimensional magnonic crystal. *Appl. Phys. Lett.* **93,** 022508 (2008).
119. Obry, B. *et al.* A micro-structured ion-implanted magnonic crystal. *Appl. Phys. Lett.* **102,** 202403 (2013).
120. Tacchi, S. *et al.* Magnetic normal modes in squared antidot array with circular holes: A combined Brillouin light scattering and broadband ferromagnetic resonance study. *IEEE Trans. Magn.* **46,** 172–178 (2010).
121. Reed, K. W., Owens, J. M. & Carter, R. L. Current status of magnetostatic reflective array filters. *Circuits Syst. Signal Process.* **4,** 157–180 (1985).
122. Karenowska, A. D., Chumak, A. V., Serga, A. A., Gregg, J. F. & Hillebrands, B. Magnonic crystal based forced dominant wavenumber selection in a spin-wave active ring. *Appl. Phys. Lett.* **96,** 082505 (2010).
123. Inoue, M. *et al.* Investigating the use of magnonic crystals as extremely sensitive magnetic field sensors at room temperature. *Appl. Phys. Lett.* **98,** 132511 (2011).
124. Karenowska, A. D. *et al.* Oscillatory energy exchange between waves coupled by a dynamic artificial crystal. *Phys. Rev. Lett.* **108,** 015505 (2012).
125. Vogel, M. *et al.* Optically-reconfigurable magnetic materials. *Nature Phys.* **11,** 487–491 (2015).
126. Chumak, A. V. *et al.* All-linear time reversal by a dynamic artificial crystal. *Nature Commun.* **1,** 141 (2010).
127. Locatelli, N., Cros, V. & Grollier, J. Spin-torque building blocks. *Nature Mater.* **13,** 11–20 (2014).
128. Kostylev, M. P., Serga, A. A., Schneider, T., Leven, B. & Hillebrands, B. Spin-wave logical gates. *Appl. Phys. Lett.* **87,** 153501 (2005).
129. Nembach, H. T., Shaw, J. M., Weiler, M., Jué, E. & Silva, T. J. Spectroscopic confirmation of linear relation between Heisenberg- and interfacial Dzyaloshinskii–Moriya-exchange in polycrystalline metal films. Preprint at http://arxiv.org/abs/1410.6243 (2014).
130. Di, K. *et al.* Direct observation of the Dzyaloshinskii–Moriya interaction in a Pt/Co/Ni film. *Phys. Rev. Lett.* **114,** 047201 (2015).
131. Tabuchi, Y. *et al.* Hybridizing ferromagnetic magnons and microwave photons in the quantum limit. *Phys. Rev. Lett.* **113,** 083603 (2014).
132. Karenowska, A. D., Patterson, A. D., Peterer, M. J., Magnússon, E. B. & Leek, P. J. Excitation and detection of propagating spin waves at the single magnon level. Preprint at http://arxiv.org/abs/1502.06263 (2015).
133. Nozaki, T. *et al.* Electric-field-induced ferromagnetic resonance excitation in an ultrathin ferromagnetic metal layer. *Nature Phys.* **8,** 491–496 (2012).
134. Khomeriki, R., Chotorlishvili, L., Malomed, B. A. & Berakdar, J. Creation and amplification of electromagnon solitons by electric field in nanostructured multiferroics. *Phys. Rev. B* **91,** 041408(R) (2015).
135. Dutta, S. *et al.* Non-volatile clocked spin wave interconnect for beyond-CMOS nanomagnet pipelines. *Sci. Rep.* **5,** 9861 (2015).
136. Urazuka, Y., Imamura, K., Oyabu, S., Tanaka, T. & Matsuyama, K. Successive logic-in-memory operation in spin wave-based devices with domain wall data coding scheme. *IEEE Trans. Magn.* **50,** 3401303 (2014).
137. Fert, A., Cros, V. & Sampaio, J. Skyrmions on the track. *Nature Nanotech.* **8,** 152–156 (2013).
138. Schutte, C. & Garst, M. Magnon-skyrmion scattering in chiral magnets. *Phys. Rev. B* **90,** 094423 (2014).

Acknowledgements

Financial support from the Deutsche Forschungsgemeinschaft (DFG) and from by EU-FET (Grant InSpin 612759) is acknowledged.

Additional information

Reprints and permissions information is available online at www.nature.com/reprints. Correspondence should be addressed to A.V.C.

Competing financial interests

The authors declare no competing financial interests.